Statistical analysis of thermal conductivity experimentally measured in water-based nanofluids

Author for correspondence:

M. Avila

e-mail: marc.avila@zarm.uni-bremen.de

J. Tielke[1], M. Maas[2,3], M. Castillo[1], K. Rezwan[2,3] and M. Avila[1,3]

[1]University of Bremen, Center of Applied Space Technology and Microgravity (ZARM), Am Fallturm, 2, 28359 Bremen, Germany
[2]University of Bremen, Advanced Ceramics, Am Biologischen Garten, 2, 28359 Bremen, Germany
[3]MAPEX Center for Materials and Processes, University of Bremen, 28359 Bremen, Germany

JT, 0000-0001-7119-5333

Nanofluids are suspensions of nanoparticles in a base heat-transfer liquid. They have been widely investigated to boost heat transfer since they were proposed in the 1990s. We present a statistical correlation analysis of experimentally measured thermal conductivity of water-based nanofluids available in the literature. The influences of particle concentration, particle size, temperature and surfactants are investigated. For specific particle materials (alumina, titania, copper oxide, copper, silica and silicon carbide), separate analyses are performed. The conductivity increases with the concentration in qualitative agreement with Maxwell's theory of homogeneous media. The conductivity also increases with the temperature (in addition to the improvement due to the increased conductivity of water). Surprisingly, only silica nanofluids exhibit a statistically significant effect of the particle size, whereby smaller particles lead to faster heat transfer. Overall, the large scatter in the experimental data prevents a compelling, unambiguous assessment of these effects. Taken together, the results of our analysis suggest that more comprehensive experimental characterizations of nanofluids are necessary to estimate their practical potential.

1. Introduction

The efficient removal of heat with circulating fluids is pivotal to applications in mechatronics, mechanical, aerospace and chemical engineering. The main limiting material property in heat transfer is the thermal conductivity (k) of the fluid, followed by the viscosity. Conventional liquids used for heat transfer, such as water or ethylene glycol, are inexpensive but exhibit low k-values. In an influential paper published in 1995, Choi & Eastman [1] proposed that 'an innovative class of heat transfer fluids can be engineered by suspending metallic nanoparticles in conventional heat transfer fluids. The resulting nanofluids are expected to exhibit high thermal conductivities'. Their experimental measurements with ethylene glycol exhibited an increase in thermal conductivity up to 20% at a volume fraction of 4% through the addition of copper oxide particles ($d \approx$ 20 nm) and spurred many theoretical and experimental investigations [2]. Several models were proposed to explain what was historically termed as anomalous heat transfer, meaning that the effective material properties of the suspension (e.g. effective viscosity and thermal conductivity of the nanofluid) could not solely account for the enhanced heat transfer [3,4]. In an influential paper, Buongiorno [5] considered many possible physical mechanisms behind convective heat transfer enhancement in nanofluids and assessed their plausibility and relative importance. He argued that Brownian motion and thermophoresis (i.e. the motion of particles along gradients of temperature) were the two only plausible mechanisms for heat transfer enhancement. Keblinski et al. [6] critically analysed some experimental datasets and concluded that effective medium theories are capable of explaining the data.

In 2009, Buongiorno et al. [7] performed an experimental benchmark study to determine the influence of the measurement technique on the experimental thermal conductivity of nanofluids. This study showed that the data scattered in a range of at least ±5% about the median, which implied that a total enhancement of a few per cent cannot be detected. Subsequently, Khanafer et al. [8] developed correlations for thermal conductivity and viscosity based on experimental data. There have been no additional benchmark studies or statistical analysis since their study. Characterization efforts have mainly focused on the analysis of the nanoparticle sizes and particle concentrations [9–13].

Recently, the state of the art in this field was reviewed by Buschmann et al. [14], who analysed several experiments on convective heat transfer with nanofluids. Their analysis supported the conclusion of Buongiorno [5] that there are no anomalies in the convective or conductive heat transfer of nanofluids. Buschmann et al. [14] argued that nanofluids can be treated as homogeneous fluids by considering their effective properties. Hence, their heat transfer can be correctly predicted by well-established correlations for pure fluids, provided that the effective thermal conductivity and the effective viscosity of the nanofluid are known. Finally, Buschmann et al. [14] pointed out that there is currently a lack of knowledge of how and why nanoparticles change the thermal conductivity of a fluid.

The observation that thermophysical properties are modified by additions of particles to a fluid dates back to the theoretical work of Maxwell in 1881 [15]. According to his Effective Medium Theory, the effective thermal conductivity of a nanofluid k_{eff} depends on the thermal conductivities of the nanoparticles k_p, thermal conductivity of the base fluid k_f, and particle fraction φ,

$$\frac{k_{eff}}{k_f} = 1 + \frac{3\varphi(k_p - k_f)}{3k_f + (1 - \varphi)(k_p - k_f)}. \tag{1.1}$$

Eapen et al. [16] argued that there may be different dispersion states in nanofluids that influence thermal conductivity, which are not considered in Maxwell's theory. For example, particles can form percolating structures at moderately low concentrations [16,17]. Through the use of a theory developed by Hashin & Shtrikman [18], Eapen et al. [16] derived the following Hashin and Shtrikman (HS)-bounds for the effective thermal conductivity of nanofluids

$$k_f \left[1 + \frac{3\varphi(k_p - k_f)}{3k_f + (1 - \varphi)(k_p - k_f)} \right] \leq k_{eff} \leq k_p \left[1 - \frac{3(1 - \varphi)(k_p - k_f)}{3k_p - \varphi(k_p - k_f)} \right]. \tag{1.2}$$

The lower HS-bound represents the well-dispersed state, where the particles are the disperse phase and the base fluid is the continuous phase, which was already described by Maxwell, see equation (1.1). Hence, in the well-dispersed state, heat is mainly transferred through the fluid. The upper HS-bound represents a state in which heat is mainly transferred between particles [16,18,19]. Specifically, at high concentrations ($\varphi \approx 1$), the base fluid becomes the dispersed phase and particles the continuous phase. Even if this limit is not realistic for e.g. spherical particles (due to close-packing), it is still useful in describing particle configurations (chains, percolation networks), which can arise even at low concentrations and result in strongly enhanced heat transfer [20].

Maxwell's and Hashin & Shtrikman's theories of suspensions do not account for the particle size, whereas the distinct feature of nanofluids is that the particles are less than 100 nm in one dimension. Vadasz [21] considered heat conduction in nanofluids and reviewed the transient-hot-wire method. He showed that by accounting for the dependence of the heat transfer coefficient on the particle size (through the particle's specific area S), the experimental data became consistent with classical theories of suspensions. However, he stated that his analysis was inconclusive and that more experimental data were required. Further experimental studies [11,22–25] showed that thermal conductivity increases linearly with increasing temperature and suggested an effect from the particle size.

Bouguerra *et al.* [20] recently showed that the effective thermal conductivity and the effective viscosity of water-based alumina nanofluids strongly depend on pH. They were able to distinguish between different dispersion states that included well-dispersed particles, the formation of percolation networks, and fully agglomerated particles, through measurements with volume concentrations between 0.2% and 2% at different pH levels. Variations of the pH modify the suspension stability through repulsive forces of electrostatic origin. An alternative to this is the use of surfactants. Depending on the choice and concentration of the surfactant, the thermal conductivity of the nanofluid may be increased or decreased [12,26–30], and to date there is no general, coherent picture as to what the effect of surfactants on the nanofluid is.

In this paper, we present a statistical correlation analysis of thermal conductivity measurements of water-based nanofluids available in the scientific literature. The aim of our analysis is to assess nanofluids for potential applications and to identify suitable nanomaterials for heat transfer. To this avail, we analyse whether the influences of particle concentration, size, temperature and surfactants on the thermal conductivity of nanofluids are statistically significant, and we quantify their relative importance.

2. Material and methods

We compiled a database with $N = 1656$ data points (experimental measurements of the thermal conductivity) from 73 publications concerned with water-based nanofluids. The data points were taken from publications in which temperature, volume concentration and particle size were fully specified. The database is given in the electronic supplementary materials and contains data for 17 different nanoparticle materials. In the first part of our analysis, all data points were considered. Subsequently, six individual materials were analysed for which there are at least four different publications available comprising $N \geq 50$ data points altogether. This was done to avoid spurious results due to small samples. The six individual materials are

- alumina (Al_2O_3, $N = 470$): [2,9,12,13,20,22–24,31–57]
- titania (TiO_2, $N = 188$) [44,50,57–63]
- copper oxide (CuO, $N = 106$) [12,22,24,44,52,56,64]
- copper (Cu, $N = 94$) [26,27,56,65,66]
- silica (SiO_2, $N = 86$) [13,32,67–72]
- silicon carbide (SiC, $N = 53$) [73–77].

Descriptive statistics for these datasets are shown in electronic supplementary materials, table S1. We note that for the analysis of copper nanofluids we excluded the study of Liu [65]. This study

features results which are very different from those of all other works for the same material. The decision to exclude them is further justified later. Here it suffices to say that as a result of excluding this, the regression significantly improves. For completeness, a comparison to the regressions with all data points (without exclusion) can be found in the electronic supplementary materials.

For the materials below, there are fewer than four publications and/or fewer than 50 data points. Thus, we did not analyse them individually, because the analysis would have little statistical significance:

— iron(III)oxide (Fe_2O_3, $N = 86$) [78,79]
— iron(II,III)oxide (Fe_3O_4, $N = 98$) [80–82]
— zinc oxide (ZnO, $N = 3$) [50]
— graphene (G, $N = 145$) [28,83,84]
— graphene oxide (GO, $N = 20$) [85]
— carbon-nanotubes (CNT, $N = 188$) [28,29]
— nanodiamond (ND, $N = 38$) [86,87]
— silver (Ag, $N = 34$) [68,70,88,89]
— iron (Fe, $N = 15$) [90]
— aluminium (Al, $N = 20$) [56]
— gold (Au, $N = 4$) [91,92].

We caution that the published data for metals have to be interpreted critically because metallic particles easily oxidize in water [93,94].

(a) Linear statistical model

We employed a linear model to statistically quantify the effect of the volume concentration φ, the temperature T and the particle size (through the specific surface S) on the normalized thermal conductivity

$$k^*(\varphi, T, S) = \frac{k_{\text{eff}}(\varphi, T, S)}{k_{\text{f}}(T)},$$ (2.1)

where $k_{\text{f}}(T)$ is the thermal conductivity of the base fluid (pure water) as a function of the temperature. Changes in the thermal conductivity of the base fluid k_f due to the addition of surfactants or changes in the pH were taken account of, if the data were specified in the respective studies. Nevertheless, most of the data are given normalized or are normalized on pure water.

Our linear statistical regression model reads

$$k^*(\varphi, T, S) = C_0 + C_\varphi \, \varphi + C_T \, T^* + C_S \, S^*,$$ (2.2)

where the coefficients C_i (with $i = \{0, \varphi, T, S\}$) were determined from linear regressions of the datasets. These coefficients are dimensionless, due to the definitions of $T^* = (T - T_{\text{ref}})/T_{\text{ref}}$ and $S^* = (S - S_0)/S_{\text{ref}}$. We chose $T_{\text{ref}} = 293$ K because most measurements found in the literature were taken at room temperature. For large particles (with specific surface $S \approx 0$), we do not expect an increase in thermal conductivity beyond Maxwell's theory, therefore we chose $S_0 = 0$ as reference. Finally, we chose $S_{\text{ref}} = 6/d_{\text{ref}}$ with $d_{\text{ref}} = 1$ nm for simplicity (with these choices the last term simplifies to $S^* = S/S_{\text{ref}} = d_{\text{ref}}/d$).

(b) Physical interpretation of the linear statistical model

Starting with Maxwell's equation (1.1) and linearizing about zero concentration ($\varphi=0$), one obtains a linear prediction of the normalized effective thermal conductivity for small concentrations

$$k^*(\varphi) = 1 + C_{\varphi,\text{Maxwell}} \, \varphi,$$ (2.3)

where

$$C_{\varphi,\text{Maxwell}} = 3 \frac{(k_{\text{p}} - k_{\text{f}})}{(k_{\text{p}} + 2k_{\text{f}})}.$$ (2.4)

Table 1. Results of the linear regressions fitted to the entire database and for each individual material, with the number of data points (N), corrected correlation coefficient (R^2), model coefficients (C_φ, C_T, C_S) and their corresponding standardized correlation coefficients (β_φ, β_T, β_S).

material	N	R^2	C_0	C_φ	β_φ	C_T	β_T	C_S	β_S
general	1656	0.29	1.031	1.81	0.39	0.51	0.27	0.092	0.34
alumina	470	0.53	1.025	1.75	0.72	0.31	0.21	0.16	0.12
titania	188	0.75	1.018	1.69	0.58	0.63	0.51	−0.19	−0.097
copper oxide	106	0.23	1.051	1.45	0.54	0.27	0.20	−0.47	−0.057
copper	94	0.43	1.059	7.46	0.72	−0.24	−0.086	0.48	0.073
silica	86	0.27	0.994	0.61	0.35	0.10	0.31	0.42	0.47
silicon carbide	53	0.68	1.082	2.97	0.70	−0.018	−0.017	−1.25	−0.25

The coefficient $C_{\varphi,\text{Maxwell}}$ increases monotonously as the thermal conductivity of the particles k_p increases. In particular, in the low conductivity limit ($k_p \ll k_f$), $C_{\varphi,\text{Maxwell}} = -1.5$, whereas in the opposite limit ($k_p \gg k_f$), $C_{\varphi,\text{Maxwell}} = 3$. Hence in the framework of the linear Maxwell's equation (2.3), $C_{\varphi,\text{Maxwell}} \in [-1.5, 3]$. This theoretical prediction can be compared with the coefficients obtained from the linear regression of (2.2) to the compiled datasets, whereby regression values with $C_\varphi > 3$ indicate higher performance than admissible in Maxwell's theory. For example, in the aforementioned experiments of Lee *et al.* [2], the heat transfer rates increased up to 20% at a volume fraction of 4% ($\varphi = 0.04$). This would imply $C_\varphi = 5$, which cannot be explained with Maxwell's theory. Furthermore, if there are no particles ($\varphi = 0$), the thermal conductivity must remain unchanged and it would be expected that the linear correlation analysis yielded values of $C_0 \approx 1$. The deviation of C_0 from unity serves as a proxy for the level of quality of the linear model and/or for the scatter of the data.

(c) Data processing and statistical methods

Analyses were performed with IBM SPSS Statistics v. 25 using regressions with the normalized thermal conductivity (k^*) as a dependent variable and φ, T^* and S^* as independent variables. All variables were entered in a single step and confidence intervals were calculated to 95%. We evaluated the corrected correlation coefficient R^2, the coefficients (C_0, C_φ, C_T, C_S), the standard deviations of the coefficients and the standardized regression coefficients ($\beta_\varphi, \beta_T, \beta_S$). The values of ($\beta_\varphi, \beta_T, \beta_S$) were calculated by subtracting the mean from the variable and dividing by its standard deviation. The larger the standardized regression coefficient of a parameter, the higher the influence of that parameter on k^*. Our analysis demonstrated that when $|\beta_i| < 0.1$ the influence of parameter i was insignificant.

Additional analyses were also carried out with subsets of the data or variations of the model, which allowed an assessment of the robustness of the data and model. For example, to verify the use of the linear regression in terms of the concentration, we restricted the data to $\varphi \leq 0.02$. The influence of surfactants was tested by performing separate regressions for the data without surfactants. Furthermore, we fitted nonlinear regressions with quadratic and cubic terms on the concentration and also with $C_0 = 1$ fixed. Detailed results for all the linear and nonlinear regressions can be found in the electronic supplementary materials.

3. Results

The result of using a linear regression to fit all data points of our database with model equation (2.2) is shown in the first row of table 1. In figure 1, the model prediction (vertical axis) is plotted against the experimentally measured normalized thermal conductivity (horizontal
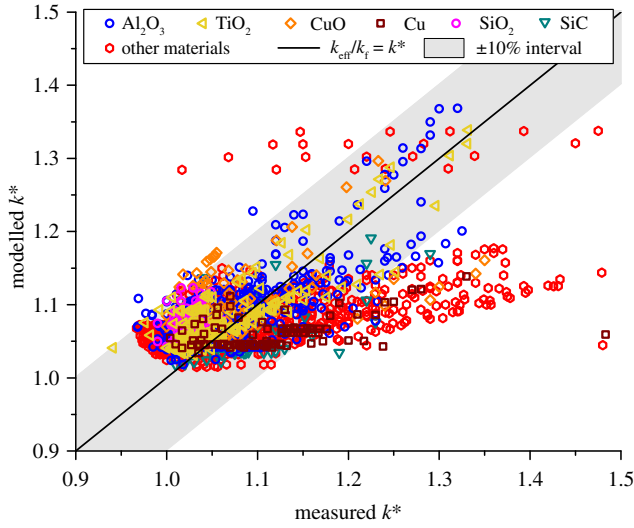
Figure 1. Experimentally measured versus modelled normalized thermal conductivity (k^*) for water-based nanofluids. The ideal values of k^* and a $\pm10\%$ interval are displayed as a solid line and a grey area, respectively. Colours are used to distinguish single materials (analysed separately) from other materials (see the legend). The model is $k^* = 1.031 + 1.81\,\varphi + 0.51\,T^* + 0.092\,S^*$ ($R^2 = 0.29$, $N = 1656$). (Online version in colour.)

axis). Data points lying along the black line exhibit perfect agreement with our linear model, equation (2.2), whereas the discrepancy is larger the further the data points are from the line. The shaded region depicts a $\pm10\%$ interval about the model prediction. The correlation coefficient is $R^2 = 0.29$ and $C_0 = 1.031$. The most significant parameter is the concentration, with $C_\varphi = 1.81$ ($\beta_\varphi = 0.39$), which is well within the bounds from the linearized Maxwell equation, $C_{\varphi,\text{Maxwell}} \in [-1.5, 3]$. The thermal conductivity also increases with increasing temperature and specific surface, with $C_T = 0.51$ ($\beta_T = 0.27$) and $C_S = 0.092$ ($\beta_S = 0.34$), respectively. These results allow a first estimation of the performance of water-based nanofluids. For example, if $d = 30$ nm at a 4% concentration and $T = 303$ K is substituted into equation (2.2)

$$k^* = C_0 + C_\varphi\,\varphi + C_T\,T^* + C_S\,S^* = 1.031 + 0.072 + 0.017 + 0.003 = 1.124,$$

a 12.4% increase in thermal conductivity is obtained (when compared to pure water at $T = 303$ K). Noteworthy, the contribution directly from the particle size (last term) is negligible.

The linear regressions to the data sets for single materials are shown in figure 2. Clearly, the scatter in the data and the goodness of the fit depend strongly on the material, which is quantified by the respective R^2 (given in the fifth column of table 1). Overall, the values of β_φ given in the fifth column of table 1 confirm that increasing the particle concentration leads to a statistically significant enhancement of the thermal conductivity for all materials analysed. In addition, there is also a significant influence of the temperature and/or surface for specific materials (see the seventh and ninth columns of table 1). In what follows, we discuss the influence of each of these three factors separately.

(a) Effect of particle concentration

The computed values of C_φ are shown in figure 3a as a function of the thermal conductivity of the particle material. The corresponding 95% confidence intervals indicate that silicon carbide nanofluids are in excellent agreement with Maxwell's prediction (equation (2.3) and lower solid line in the figure), whereas silica, alumina, titania and copper oxide nanofluids are below it. Only copper nanofluids appear to exceed Maxwell's prediction. Overall, the discrepancy with
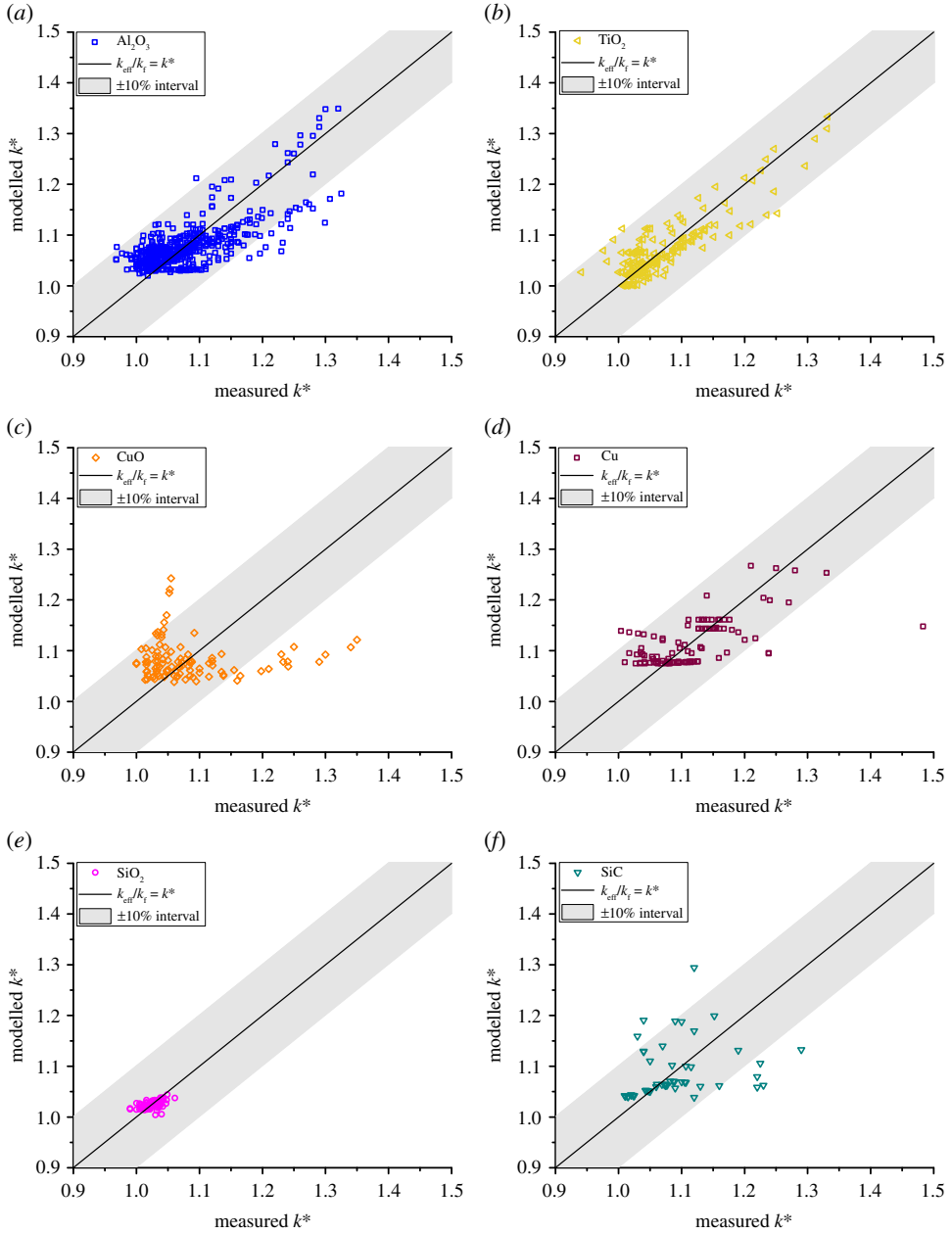
Figure 2. Experimentally measured versus modelled normalized thermal conductivity (k^*). The ideal values of k^* and a $\pm10\%$ interval are displayed as a solid line and a grey area, respectively. (*a*) Alumina with $N = 470$ and $k^* = 1.025 + 1.75\,\varphi + 0.31\,T^* + 0.16\,S^*$ ($R^2 = 0.53$). (*b*) Titania with $N = 188$ and $k^* = 1.018 + 1.69\,\varphi + 0.63\,T^* - 0.19\,S^*$ ($R^2 = 0.75$). (*c*) Copper oxide with $N = 106$ and $k^* = 1.051 + 1.45\,\phi + 0.27\,T - 0.47\,S^*$ ($R^2 = 0.23$). (*d*) Copper with $N = 94$ and $k^* = 1.059 + 7.46\,\phi + -0.24\,T + 0.48\,S^*$ ($R^2 = 0.43$). (*e*) Silica with $N = 86$ and $k^* = 0.994 + 0.61\,\phi + 0.10\,T^* + 0.42\,S^*$ ($R^2 = 0.27$). (*f*) Silicon carbide with $N = 53$ and $k^* = 1.082 + 2.97\,\varphi + -0.018\,T^* - 1.25\,S^*$ ($R^2 = 0.68$). (Online version in colour.)

Maxwell's prediction is not large in view of the large scatter in the datasets. By linearizing the upper HS-bound of equation (1.2), we obtained an upper bound for C_φ (upper solid line in figure 3*a*). This upper bound embraces all possible dispersion states and is satisfied also by copper.
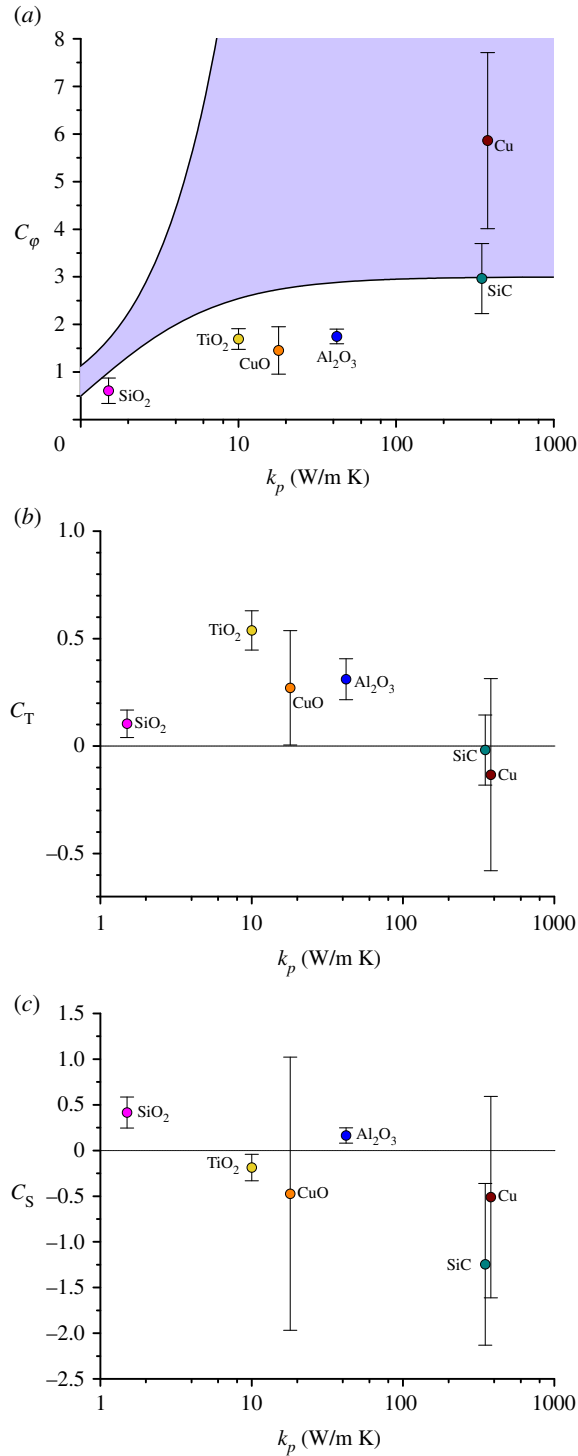
Figure 3. The coloured symbols show the values of the model coefficient C_i (with corresponding 95% confidence-interval, shown as error-bars) as a function of the thermal conductivity k_p of each material. (a) Concentration coefficients C_φ. The linearized HS-bounds are displayed as solid black line. The lower bound is given by the linearized Maxwell equation (2.3), whereas the upper HS-bound was calculated by linearizing the right-hand side of equation (1.2) (with $\varphi\ k_p/k_f = 0$). (b) Temperature coefficients C_T. (c) Surface coefficients C_S. (Online version in colour.)

(b) Effect of nanofluid temperature

The computed values of C_T for single materials are shown in figure 3b. Increasing the temperature in titania nanofluids enhances the thermal conductivity significantly and strongly. For alumina and copper oxide nanofluids, the increase in thermal conductivity is less pronounced and also less significant. For silica the effect is significant, but the performance increase is even weaker. Finally, there is no significant influence of temperature on the thermal conductivity for copper and silicon carbide nanofluids, which is due to a lack of experimental measurements for a sufficiently large range of temperatures (see electronic supplementary material, table S1, fig. S2).

(c) Effect of the particle size

The computed values of C_S are shown in figure 3c. A strong effect of the particle size is found only in silica nanofluids ($C_S = 0.42$, $\beta_S = 0.47$). For alumina nanofluids, the particle size has a mildly significant and weak effect. In both cases, reducing the particle size appears to enhance the thermal conductivity. By contrast, for silicon carbide nanofluids the computed coefficient is negative ($C_S = -1.25$), suggesting that increasing the particle size leads to higher thermal conductivity. However, the large scatter in the data for this material (see the corresponding confidence intervals in figure 3c) does not allow a conclusive statement. For copper oxide and copper nanofluids, the effect is statistically insignificant, which may be attributed to the absence of variation in particle size in the experimental measurements available (see electronic supplementary material, table S1 and figure S2).

The case of titania is more complicated to interpret. Here the experimental measurements span a wide range of particle sizes, yet the particle-size effect is insignificant if all data are used. If only the measurements without surfactant are considered in the statistical analysis, the particle size appears to have a very strong and significant influence, with $C_S = 1.931$ and $\beta_S = 0.367$. The descriptive statistics and boxplot diagram in the supplementary material (see figures S2 and S4 therein) show an irregular distribution of the measured particle sizes, with most measurements for $d = 21$ nm and a few for 100 nm. This may result in the significant regression coefficients.

(d) Effect of surfactants

Out of $N = 1656$ data points, 1038 data points (62%) were obtained in suspensions without surfactants, whereas 618 (38%) data points were obtained with surfactants. Half of these data points (309) were from surfactant concentrations of less than 1.67 wt%, the rest with concentrations higher than 10 wt% (225 data points) or provided no information about the concentration (84 data points). Descriptive statistics and corresponding boxplots can be found in the electronic supplementary material, §2. Depending on the type of the surfactant and concentration, the thermal conductivity of both, the base fluid and the nanofluid, may increase or decrease [12,26–29]. Because of the heterogeneity of the measurements with surfactants (in type and concentration), it would be meaningful to analyse data with similar surfactant configurations together. However, this would lead to small data subsets and would prevent statistically significant analyses. Hence, in this work, we statistically investigated the effect of surfactants by performing regressions of the data points obtained without surfactants (separately for each material), and then comparing the results to those presented in the previous sections (with and without surfactants).

The data for copper were all obtained with surfactants except for the study of Liu *et al.* [65]; this is the reason why their work was excluded from the analysis for copper. For SiO_2 and SiC nanofluids, no surfactants were used. Hence the effect of surfactants cannot be investigated for these materials, as no comparisons (with/without surfactants) are possible. Still, we stress that the results for copper reveal a C_φ beyond Maxwell's theory in contrast to the other materials and insignificant C_T and C_S coefficients with large error-bars.

Comparisons were possible for Al_2O_3 and CuO, with (405/470) and (94/106) data points obtained without surfactants, respectively. The changes in the regressions of alumina and copper oxide without surfactants lie within the 95% intervals of the regression for the whole datasets. Major changes occurred in the case of TiO_2. Out of $N = 188$ data points, 83 were obtained without surfactants. The concentration coefficient C_φ increases and nearly approaches Maxwell's prediction. The coefficients C_T and C_S increase beyond the 95% interval of the whole data set, whereas C_0 decreases.

Overall it can be concluded that while surfactants are expected to change the stability and the thermal conductivity of nanofluids, no conclusive statements can be made with the data available in the literature.

4. Discussion

Buongiorno *et al.* [7] pointed out already one decade ago that nanofluid data in the literature exhibit large scatter (±5% about the median). A first critical statistical analysis of the scatter in the experimental data was done by Khanafer & Vafai [8]. Our statistical analysis extends and updates their analyses and confirms that the scatter in the different datasets is very large, as illustrated by the regression coefficients $R^2 \in [0.23, 0.75]$. In line with Buongiorno *et al.* [7], we attribute the large scatter in the data to two factors. First, the experimental determination of thermophysical properties (e.g. thermal conductivity) of fluids is known to be susceptible of errors (even for pure fluids). Chirico *et al.* [95] reviewed thermophysical data from five major journals and found errors in nearly one-third of all publications. The most common problems were data with omitted uncertainties and the use of volume-based units [95]. Furthermore, in many publications the particle parameters (e.g. the size) were directly taken from the manufacturers, which is another source of error. Second, the characterizations of the nanofluids performed in the literature are often insufficient and additional variables need to be taken into account. Nieto de Castro *et al.* [96] considered the different factors influencing the thermal conductivity of nanofluids and emphasized the need for accurate, comparable measurements including stability characterizations (see also [97,98]).

(a) Dispersion state

The stability of nanofluids depends on their preparation, i.e. on the use of surfactants and/or the pH value of the fluid. For example, the colloidal stabilization of titania, alumina and other oxidic particles highly depends on pH [20], whereas hydrophobic particles (e.g. silicon carbide) agglomerate without the addition of dispersing agents [6,99,100]. Hence the surfactant itself and the concentration must be selected very carefully to maximize the thermal conductivity. Owing to the heterogeneity in surfactant type and concentration (and particle material and size) used across studies, it is difficult to compare data and draw general conclusions from them. Hence, despite the widespread use of surfactants, the results are ambiguous at best. Many studies suggest improved thermal conductivity, whereas others suggest the opposite [12,26–29]. The copper nanofluids in the literature were synthesized with the use of surfactants. In most studies, the concentration of surfactants was above the critical micelle concentration, possibly generating networks of micelles in the nanofluid. Hence the high value of C_φ obtained for copper may arise from a dispersion state different than well-dispersed particles. We note however that micellar aggregates, worm-like micelles and network structures increase the viscosity of the nanofluid [30,101]. Thus, the use of high surfactant concentrations may lead to high thermal conductivities, but may be rather unfavourable for the application of nanofluids.

Our analysis employs a linear regression to assess the importance of concentration, temperature and specific surface. This precludes an investigation of combined effects, whereas surface (particle-size) effects may depend on the concentration. Unfortunately, the quality and quantity of the published data do not currently allow for a statistically significant analysis of such combined effects via the inclusion of nonlinear terms (e.g. of the form $C_{\varphi,S}\, \varphi\, S^*$). We note

however that we did not find any significant cross-correlations between variables. The aging and stability of the nanofluid, which change the dispersion state, could not be included in our statistical analysis, because these factors are seldom described in sufficient detail in published data [7,102,103]. For the same reason, we could not analyse the dependence of the effective viscosity on concentration, temperature and size of the nanoparticles.

The viscosity is crucial in heat transfer applications and complex structures, such as particle clusters or percolation networks, dramatically increase the viscosity of suspensions. Bouguerra *et al.* [20] have shown that for alumina nanofluids the well-dispersed regime (when available), is the preferred one for heat transfer applications. Studies employing molecular dynamics simulations have also shown that clustering influences the thermal conductivity of nanofluids [104–106], and increases their viscosity [104,105]. Tahmooressi *et al.* [106] showed for nanoparticles at high concentrations ($\varphi = 0.1$) that the agglomeration of nanoparticles into small clusters may be more efficient towards high thermal conductivities than well-dispersed particles or percolating networks. This is in line with the experimental observations of Bouguerra *et al.* [20] measuring higher thermal conductivities for percolation than for dispersed particles. Clearly, simultaneous measurements of thermal conductivity and viscosity, and direct measurements of the state of dispersion of the nanofluid would be very useful. Here the determination of the diffusion coefficient and the size of the hydration layer would help [19,107,108].

(b) Regressions with $C_0 = 1$

We also fitted all datasets discussed above, but imposing $C_0 = 1$ in equation (2.2). The results are shown in electronic supplementary material, table S6a–g and figures S5–S7. For silica nanofluids, the results do not change much when $C_0 = 1$ is imposed. For all other particle materials, imposing $C_0 = 1$ leads to an increase in the values of C_φ, C_T and C_S. This is because for all these materials $C_0 > 1$ in the linear regressions. In fact, the larger the value of C_0 in the linear regression, the larger the increase of the other coefficients when $C_0 = 1$ is set. For silicon carbide, copper oxide and copper nanofluids, the value of C_S even changes from negative to positive. Hence nothing can be said about particle size for these nanofluids. In both linear and nonlinear analyses, the 95% confidence intervals for the surface coefficient C_S reflect the large scatter in the data regarding particle size effects. Overall, it can be concluded that setting $C_0 = 1$ does not qualitatively change the results of our analysis, but rather fortifies our findings and our assessment of the data quality.

(c) Analysis for small concentrations $\varphi \leq 0.02$

We analysed the data for concentrations below 2% separately to assess the validity of the linear assumption for the concentration in our statistical regression model. We found statistically identical results for silica, silicon carbide and copper. For copper oxide, titania and alumina (see electronic supplementary material, §2.1 and figure S3) the (relative) performance is better at low concentrations. For alumina, there is then perfect agreement with Maxwell, whereas titania and copper oxide are above the Maxwell curve, but with confidence intervals nearly touching it. It can be concluded that higher concentrations decrease the (relative) performance, possibly due to unfavourable agglomeration effects (e.g. [20]).

5. Conclusion and outlook

Our statistical analysis shows that the experimentally measured thermal conductivity of water-based nanofluids increases approximately linearly with the particle concentration. Within statistical uncertainty, this increase can be accounted for by Maxwell's Effective Medium Theory for all materials. A possible exception may be copper nanofluids, although more experiments are necessary to assess their performance and the role of surfactants. A linear increase of

the conductivity with the temperature was observed for all materials in which measurements covering sufficiently large temperature ranges are available. Finally, only silica nanofluids exhibit statistically significant, strong particle-size effects, which makes this scarcely investigated material interesting for fundamental investigations. In particular, in silica nanofluids, reducing the particle size (at constant concentration) leads to higher conductivity. Their performance is however low (compared to other nanofluids) because of their low value of C_φ.

In the view of the detrimental effect of the increased viscosity and of stability issues, we suggest that the potential of nanofluids in engineering practice is limited. The main advantage of nanofluids, when compared to suspensions of larger particles, is their reduced sedimentation speed. We conclude that the large scatter found in the experimental measurements makes it difficult to test and compare theories for the effective thermal conductivity of water-based nanofluids. More comprehensive and precise characterizations, including the analysis of the dispersion state and of the stability on nanofluids (e.g. depending on the surfactant), are needed to quantify the sources of the data scatter. We believe that an improvement of the state of the art can only be achieved by ensuring the reproducibility of results with *a priori* identical conditions in different research groups. Silica nanoparticles are usually homogeneous in their size, are easy to handle and are sufficiently stable in dispersion. Hence, silica nanofluids are good candidates to precisely quantify the effects of particle size and dispersion stability on nanofluids. Copper nanofluids exhibit high thermal conductivities, but in order to compare their performance to other materials, it would be necessary to stabilize them with small concentrations of surfactant (below the critical micelle concentration). Unfortunately, this is challenging because metal nanoparticles rapidly oxidize and agglomerate without surfactants [109].

Finally, we suggest that more sophisticated statistical analyses [110,111] could be employed to shed light on the source of the variability in the measured thermal conductivity of nanofluids. We will investigate possible factors in future work.

References

1. Choi SUS, Eastman J. 1995 Enhancing thermal conductivity of fluids with nanoparticles. In *Developments and applications of non-Newtonian flows* (eds DA Siginer, HP Wang), pp. 99–105, FED-vol. 231/MD-vol. 66. New York, NY: ASME International Mechanical Engineering.
2. Lee S, Choi SUS, Li S, Eastman JA. 1999 Measuring thermal conductivity of fluids containing oxide nanoparticles. *J. Heat Transfer* **121**, 280–289. (doi:10.1115/1.2825978)
3. Pak BC, Cho YI. 1998 Hydrodynamic and heat transfer study of dispersed fluids with submicron metallic oxide particles. *Exp. Heat Transfer* **11**, 151–170. (doi:10.1080/08916159808946559)
4. Eastman JA, Phillpot SR, Choi SUS, Keblinski P. 2004 Thermal transport in nanofluids. *Annu. Rev. Mater. Res.* **34**, 219–246. (doi:10.1146/annurev.matsci.34.052803.090621)
5. Buongiorno J. 2005 Convective transport in nanofluids. *J. Heat Transfer* **128**, 240–250. (doi:10.1115/1.2150834)
6. Keblinski P, Prasher R, Eapen J. 2008 Thermal conductance of nanofluids: is the controversy over? *J. Nanopart. Res.* **10**, 1089–1097. (doi:10.1007/s11051-007-9352-1)

7. Buongiorno J *et al.* 2009 A benchmark study on the thermal conductivity of nanofluids. *J. Appl. Phys.* **106**, 94312. (doi:10.1063/1.3245330)

8. Khanafer K, Vafai K. 2011 A critical synthesis of thermophysical characteristics of nanofluids. *Int. J. Heat Mass Transfer* **54**, 4410–4428. (doi:10.1016/j.ijheatmasstransfer.2011.04.048)

9. Gowda R, Sun H, Wang P, Charmchi M, Gao F, Gu Z, Budhlall B. 2010 Effects of particle surface charge, species, concentration, and dispersion method on the thermal conductivity of nanofluids. *Adv. Mech. Eng.* **2**, 807610. (doi:10.1155/2010/807610)

10. Fan J, Wang L. 2011 Heat conduction in nanofluids: structure–property correlation. *Int. J. Heat Mass Transfer* **54**, 4349–4359. (doi:10.1016/j.ijheatmasstransfer.2011.05.009)

11. Lee JH, Lee SH, Pil Jang S. 2014 Do temperature and nanoparticle size affect the thermal conductivity of alumina nanofluids? *Appl. Phys. Lett.* **104**, 161908. (doi:10.1063/1.4872164)

12. Gangadevi R, Vinayagam BK, Senthilraja S. 2018 Effects of sonication time and temperature on thermal conductivity of CuO/water and Al_2O_3/water nanofluids with and without surfactant. *Mater. Today: Proc.* **5**(2, Part 3), 9004–9011. (doi:10.1016/j.matpr.2017.12.347)

13. Mikkola V, Puupponen S, Granbohm H, Saari K, Ala-Nissila T, Seppälä A. 2018 Influence of particle properties on convective heat transfer of nanofluids. *Int. J. Therm. Sci.* **124**, 187–195. (doi:10.1016/j.ijthermalsci.2017.10.015)

14. Buschmann MH, Azizian R, Kempe T, Juliá JE, Martínez-Cuenca R, Sundén B, Wu Z, Seppälä A, Ala-Nissila T. 2018 Correct interpretation of nanofluid convective heat transfer. *Int. J. Therm. Sci.* **129**, 504–531. (doi:10.1016/j.ijthermalsci.2017.11.003)

15. Maxwell JC. 1881 *A treatise on electricity and magnetism*, 2nd edn. Oxford, UK: Clarendon Press.

16. Eapen J, Rusconi R, Piazza R, Yip S. 2010 The classical nature of thermal conduction in nanofluids. *J. Heat Transfer* **132**, 102 402–102 414. (doi:10.1115/1.4001304)

17. Carson JK, Lovatt SJ, Tanner DJ, Cleland AC. 2005 Thermal conductivity bounds for isotropic, porous materials. *Int. J. Heat Mass Transfer* **48**, 2150–2158. (doi:10.1016/j.ijheatmasstransfer.2004.12.032)

18. Hashin Z, Shtrikman S. 1962 A variational approach to the theory of the effective magnetic permeability of multiphase materials. *J. Appl. Phys.* **33**, 3125–3131. (doi:10.1063/1.1728579)

19. Mugica I, Poncet S. 2020 A critical review of the most popular mathematical models for nanofluid thermal conductivity. *J. Nanopart. Res.* **22**, 113. (doi:10.1007/s11051-020-4776-y)

20. Bouguerra N, Poncet S, Elkoun S. 2018 Dispersion regimes in alumina/water-based nanofluids: simultaneous measurements of thermal conductivity and dynamic viscosity. *Int. Commun. Heat Mass Transfer* **92**, 51–55. (doi:10.1016/j.icheatmasstransfer.2018.02.015)

21. Vadasz P. 2006 Heat conduction in nanofluid suspensions. *J. Heat Transfer* **128**, 465–477. (doi:10.1115/1.2175149)

22. Das SK, Putra N, Thiesen P, Roetzel W. 2003 Temperature dependence of thermal conductivity enhancement for nanofluids. *J. Heat Transfer* **125**, 567–574. (doi:10.1115/1.1571080)

23. Chon CH, Kihm KD, Lee SP, Choi SUS. 2005 Empirical correlation finding the role of temperature and particle size for nanofluid (Al_2O_3) thermal conductivity enhancement. *Appl. Phys. Lett.* **87**, 153107. (doi:10.1063/1.2093936)

24. Li CH, Peterson GP. 2006 Experimental investigation of temperature and volume fraction variations on the effective thermal conductivity of nanoparticle suspensions (nanofluids). *J. Appl. Phys.* **99**, 84314. (doi:10.1063/1.2191571)

25. Li CH, Peterson GP. 2007 The effect of particle size on the effective thermal conductivity of Al_2O_3-water nanofluids. *J. Appl. Phys.* **101**, 44312. (doi:10.1063/1.2436472)

26. Yang JC, Li FC, Zhou WW, He YR, Jiang BC. 2012 Experimental investigation on the thermal conductivity and shear viscosity of viscoelastic-fluid-based nanofluids. *Int. J. Heat Mass Transfer* **55**, 3160–3166. (doi:10.1016/j.ijheatmasstransfer.2012.02.052)

27. Li XF, Zhu DS, Wang XJ, Wang N, Gao JW, Li H. 2008 Thermal conductivity enhancement dependent pH and chemical surfactant for $Cu - H_2O$ nanofluids. *Thermochim. Acta* **469**, 98–103. (doi:10.1016/j.tca.2008.01.008)

28. Kim S, Tserengombo B, Choi SH, Noh J, Huh S, Choi B, Chung H, Kim J, Jeong H. 2018 Experimental investigation of dispersion characteristics and thermal conductivity of various surfactants on carbon based nanomaterial. *Int. Commun. Heat Mass Transfer* **91**, 95–102. (doi:10.1016/j.icheatmasstransfer.2017.12.011)

29. Nasiri A, Shariaty-Niasar M, Rashidi A, Amrollahi A, Khodafarin R. 2011 Effect of dispersion method on thermal conductivity and stability of nanofluid. *Exp. Therm Fluid Sci.* **35**, 717–723. (doi:10.1016/j.expthermflusci.2011.01.006)

30. Cao F, Liu Y, Xu J, He Y, Hammouda B, Qiao R, Yang B. 2015 Probing nanoscale thermal transport in surfactant solutions. *Sci. Rep.* **5**, 16040. (doi:10.1038/srep16040)

31. Beck MP, Yuan Y, Warrier P, Teja AS. 2009 The effect of particle size on the thermal conductivity of alumina nanofluids. *J. Nanopart. Res.* **11**, 1129–1136. (doi:10.1007/s11051-008-9500-2)

32. Bowers J, Cao H, Qiao G, Li Q, Zhang G, Mura E, Ding Y. 2018 Flow and heat transfer behaviour of nanofluids in microchannels. *Prog. Nat. Sci.: Mater. Int.* **28**, 225–234. (doi:10.1016/j.pnsc.2018.03.005)

33. Chandrasekar M, Suresh S. 2011 Experiments to explore the mechanisms of heat transfer in nanocrystalline alumina/water nanofluid under laminar and turbulent flow conditions. *Exp. Heat Transf.* **24**, 234–256. (doi:10.1080/08916152.2010.523809)

34. El-Brolossy TA, Saber O. 2013 Non-intrusive method for thermal properties measurement of nanofluids. *Exp. Therm. Fluid Sci.* **44**, 498–503. (doi:10.1016/j.expthermflusci.2012.08.011)

35. Hemmat Esfe M, Saedodin S, Mahian O, Wongwises S. 2014 Thermal conductivity of Al_2O_3/water nanofluids. *J. Therm. Anal. Calorim.* **117**, 675–681. (doi:10.1007/s10973-014-3771-x)

36. Heyhat MM, Kowsary F, Rashidi AM, Esfehani SAV, Amrollahi A. 2012 Experimental investigation of turbulent flow and convective heat transfer characteristics of alumina water nanofluids in fully developed flow regime. *Int. Commun. Heat Mass Transfer* **39**, 1272–1278. (doi:10.1016/j.icheatmasstransfer.2012.06.024)

37. Ho CJ, Lin YJ. 2014 Turbulent forced convection effectiveness of alumina-water nanofluid in a circular tube with elevated inlet fluid temperatures: an experimental study. *Int. Commun. Heat Mass Transfer* **57**, 247–253. (doi:10.1016/j.icheatmasstransfer.2014.08.017)

38. Hong J, Kim D. 2012 Effects of aggregation on the thermal conductivity of alumina/water nanofluids. *Thermochim. Acta* **542**(SI), 28–32. (doi:10.1016/j.tca.2011.12.019)

39. Iacobazzi F, Milanese M, Colangelo G, Lomascolo M, de Risi A. 2016 An explanation of the Al_2O_3 nanofluid thermal conductivity based on the phonon theory of liquid. *Energy* **116**, 786–794. (doi:10.1016/j.energy.2016.10.027)

40. Kayhani MH, Nazari M, Soltanzadeh H, Heyhat MM, Kowsary F. 2012 Experimental analysis of turbulent convective heat transfer and pressure drop of Al_2O_3/water nanofluid in horizontal tube. *Micro & Nano Lett.* **7**, 223–227. (doi:10.1049/mnl.2011.0706)

41. Kim CK, Lee GJ, Rhee CK. 2012 A study on heat transfer characteristics of spherical and fibrous alumina nanofluids. *Thermochim. Acta* **542**, 33–36. (doi:10.1016/j.tca.2011.12.016)

42. Kumar N, Sonawane SS, Sonawane SH. 2018 Experimental study of thermal conductivity, heat transfer and friction factor of Al_2O_3 based nanofluid. *Int. Commun. Heat Mass Transfer* **90**, 1–10. (doi:10.1016/j.icheatmasstransfer.2017.10.001)

43. Murshed SMS, Leong KC, Yang C. 2008 Investigations of thermal conductivity and viscosity of nanofluids. *Int. J. Therm. Sci.* **47**, 560–568. (doi:10.1016/j.ijthermalsci.2007.05.004)

44. Nair V, Parekh AD, Tailor PR. 2018 Water-based Al_2O_3, CuO and TiO_2 nanofluids as secondary fluids for refrigeration systems: a thermal conductivity study. *J. Brazilian Soc. Mech. Sci. Eng.* **40**, 262. (doi:10.1007/s40430-018-1177-6)

45. Oh DW, Jain A, Eaton JK, Goodson KE, Lee JS. 2008 Thermal conductivity measurement and sedimentation detection of aluminum oxide nanofluids by using the 3ω method. *Int. J. Heat Fluid Flow* **29**, 1456–1461. (doi:10.1016/j.ijheatfluidflow.2008.04.007)

46. Ruan B, Jacobi AM. 2011 Investigation on intertube falling-film heat transfer and mode transitions of aqueous-alumina nanofluids. *J. Heat Transf.-Trans. SME* **133**, 051501-1–11. (doi:10.1115/1.4002980)

47. Rudyak VY, Minakov AV, Krasnolutskii SL. 2016 Physics and mechanics of heat exchange processes in nanofluid flows. *Phys. Mesomech.* **19**, 298–306. (doi:10.1134/S1029959916030085)

48. Said Z, Sajid MH, Saidur R, Rahim NA, Bhuiyan MHU. 2014 Rheological behaviour and the hysteresis phenomenon of Al_2O_3 nanofluids. *Mater. Res. Innov.* **18**(S6), 47–50. (doi:10.1179/1432891714Z.000000000930)

49. Teng TP, Hung YH, Teng TC, Mo HE, Hsu HG. 2010 The effect of alumina/water nanofluid particle size on thermal conductivity. *Appl. Therm. Eng.* **30**, 2213–2218. (doi:10.1016/j.applthermaleng.2010.05.036)

50. Topuz A, Engin T, Alper Özalp A, Erdoğan B, Mert S, Yeter A. 2018 Experimental investigation of optimum thermal performance and pressure drop of water-based Al_2O_3, TiO_2 and ZnO nanofluids flowing inside a circular microchannel. *J. Therm. Anal. Calorim.* **131**, 2843–2863. (doi:10.1007/s10973-017-6790-6)

51. Zhu D, Li X, Wang N, Wang X, Gao J, Li H. 2009 Dispersion behavior and thermal conductivity characteristics of $Al_2O_3 - H_2O$ nanofluids. *Curr. Appl. Phys.* **9**, 131–139. (doi:10.1016/j.cap.2007.12.008)

52. Mintsa HA, Roy G, Nguyen CT, Doucet D. 2009 New temperature dependent thermal conductivity data for water-based nanofluids. *Int. J. Therm. Sci.* **48**, 363–371. (doi:10.1016/j.ijthermalsci.2008.03.009)

53. Modi M, Kangude P, Srivastava A. 2020 Performance evaluation of alumina nanofluids and nanoparticles-deposited surface on nucleate pool boiling phenomena. *Int. J. Heat Mass Transfer* **146**, 118833. (doi:10.1016/j.ijheatmasstransfer.2019.118833)

54. Gavili A, Isfahani T. 2019 Experimental investigation of transient heat transfer coefficient in natural convection with Al_2O_3-nanofluids. *Heat Mass Transfer.* **56**, 901–911. (doi:10.1007/s00231-019-02752-5)

55. Khurana D, Subudhi S. 2019 Forced convection of Al_2O_3/water nanofluids with simple and modified spiral tape inserts. *Heat Mass Transfer.* **55**, 2831–2843. (doi:10.1007/s00231-019-02629-7)

56. Patel HE, Sundararajan T, Das SK. 2010 An experimental investigation into the thermal conductivity enhancement in oxide and metallic nanofluids. *J. Nanopart. Res.* **12**, 1015–1031. (doi:10.1007/s11051-009-9658-2)

57. Vakilinejad A, Aroon MA, Al-Abri M, Bahmanyar H, Myint MTZ, Vakili-Nezhaad GR. 2018 Experimental and theoretical investigation of thermal conductivity of some water-based nanofluids. *Chem. Eng. Commun.* **205**, 610–623. (doi:10.1080/00986445.2017.1407922)

58. Das PK, Mallik AK, Ganguly R, Santra AK. 2018 Stability and thermophysical measurements of TiO_2 (anatase) nanofluids with different surfactants. *J. Mol. Liq.* **254**, 98–107. (doi:10.1016/j.molliq.2018.01.075)

59. Duangthongsuk W, Wongwises S. 2009 Measurement of temperature-dependent thermal conductivity and viscosity of TiO_2-water nanofluids. *Exp. Therm Fluid Sci.* **33**, 706–714. (doi:10.1016/j.expthermflusci.2009.01.005)

60. Oliveira LR, Silva ACA, Dantas NO, Bandarra Filho EP. 2017 Thermophysical properties of TiO_2-PVA/water nanofluids. *Int. J. Heat Mass Transfer* **115**, 795–808. (doi:10.1016/j.ijheatmasstransfer.2017.07.094)

61. Said Z, Saidur R, Hepbasli A, Rahim NA. 2014 New thermophysical properties of water based TiO_2 nanofluid–the hysteresis phenomenon revisited. *Int. Commun. Heat Mass Transfer* **58**, 85–95. (doi:10.1016/j.icheatmasstransfer.2014.08.034)

62. Anbu S, Venkatachalapathy S, Suresh S. 2019 Convective heat transfer studies on helically corrugated tubes with spiraled rod inserts using TiO_2/DI water nanofluids. *J. Therm. Anal. Calorim.* **137**, 849–864. (doi:10.1007/s10973-019-08008-y)

63. Fedele L, Colla L, Bobbo S. 2012 Viscosity and thermal conductivity measurements of water-based nanofluids containing titanium oxide nanoparticles. *Int. J. Refrig* **35**, 1359–1366. (doi:10.1016/j.ijrefrig.2012.03.012)

64. Singh Sokhal G, Gangacharyulu D, Bulasara VK. 2018 Influence of copper oxide nanoparticles on the thermophysical properties and performance of flat tube of vehicle cooling system. *Vacuum* **157**, 268–276. (doi:10.1016/j.vacuum.2018.08.048)

65. Liu MS, Lin MCC, Tsai CY, Wang CC. 2006 Enhancement of thermal conductivity with Cu for nanofluids using chemical reduction method. *Int. J. Heat Mass Transfer* **49**, 3028–3033. (doi:10.1016/j.ijheatmasstransfer.2006.02.012)

66. Saterlie M, Sahin H, Kavlicoglu B, Liu Y, Graeve O. 2011 Particle size effects in the thermal conductivity enhancement of copper-based nanofluids. *Nanoscale Res. Lett.* **6**, 217. (doi:10.1186/1556-276X-6-217)

67. Guo W, Li G, Zheng Y, Dong C. 2018 Measurement of the thermal conductivity of SiO_2 nanofluids with an optimized transient hot wire method. *Thermochim. Acta* **661**, 84–97. (doi:10.1016/j.tca.2018.01.008)

68. Kang HU, Kim SH, Oh JM. 2006 Estimation of thermal conductivity of nanofluid using experimental effective particle volume. *Exp. Heat Transf.* **19**, 181–191. (doi:10.1080/08916150600619281)

69. Ajeel RK, Salim WI, Sopian K, Yusoff MZ, Hasnan K, Ibrahim A, Al-Waeli AH. 2019 Turbulent convective heat transfer of silica oxide nanofluid through corrugated channels: an experimental and numerical study. *Int. J. Heat Mass Transfer* **145**, 118806. (doi:10.1016/j.ijheatmasstransfer.2019.118806)

70. Ardekani AM, Kalantar V, Heyhat MM. 2019 Experimental study on the flow and heat transfer characteristics of Ag/water and SiO_2/water nanofluids flows in helically coiled tubes. *J. Therm. Anal. Calorim.* **137**, 779–790. (doi:10.1007/s10973-018-08001-x)

71. Manay E, Mandev E. 2019 Experimental investigation of mixed convection heat transfer of nanofluids in a circular microchannel with different inclination angles. *J. Therm. Anal. Calorim.* **135**, 887–900. (doi:10.1007/s10973-018-7463-9)

72. Rejvani M, Alipour A, Vahedi SM, Chamkha AJ, Wongwises S. 2019 Optimal characteristics and heat transfer efficiency of SiO_2/water nanofluid for application of energy devices: a comprehensive study. *Int. J. Energy Res.* **43**, 8548–8571. (doi:10.1002/er.4854)

73. Singh D, Timofeeva E, Yu W, Routbort J, France D, Smith D, Lopez-Cepero JM. 2009 An investigation of silicon carbide-water nanofluid for heat transfer applications. *J. Appl. Phys.* **105**, 64306. (doi:10.1063/1.3082094)

74. Chen W, Zou C, Li X, Li L. 2017 Experimental investigation of SiC nanofluids for solar distillation system: stability, optical properties and thermal conductivity with saline water-based fluid. *Int. J. Heat Mass Transfer* **107**, 264–270. (doi:10.1016/j.ijheatmasstransfer.2016.11.048)

75. Manna O, Singh S, Paul G. 2012 Enhanced thermal conductivity of nano-SiC dispersed water based nanofluid. *Bull. Mater. Sci.* **35**, 707–712. (doi:10.1007/s12034-012-0366-7)

76. Ponnada S, Subrahmanyam T, Naidu SV. 2019 An experimental investigation on heat transfer and friction factor of Silicon Carbide/water nanofluids in a circular tube. *Energy Procedia* **158**, 5156–5161. (doi:10.1016/j.egypro.2019.01.682)

77. Xie H, Wang J, Xi T, Liu Y. 2002 Thermal conductivity of suspensions containing nanosized sic particles. *Int. J. Thermophys.* **23**, 571–580. (doi:10.1023/A:1015121805842)

78. Zouli N, Said IA, Al-Dahhan M. 2019 Enhancement of thermal conductivity and local heat transfer coefficients using Fe_2O_3/water nanofluid for improved thermal desalination processes. *J. Nanofluids* **8**, 1103–1122. (doi:10.1166/jon.2019.1653)

79. Agarwal R, Verma K, Agrawal NK, Singh R. 2019 Comparison of experimental measurements of thermal conductivity of Fe_2O_3 nanofluids against standard theoretical models and artificial neural network approach. *J. Mater. Eng. Perform.* **28**, 4602–4609. (doi:10.1007/s11665-019-04202-z)

80. Abareshi M, Goharshadi EK, Mojtaba Zebarjad S, Khandan Fadafan H, Youssefi A. 2010 Fabrication, characterization and measurement of thermal conductivity of Fe_3O_4 nanofluids. *J. Magn. Magn. Mater.* **322**, 3895–3901. (doi:10.1016/j.jmmm.2010.08.016)

81. Ebrahimi S, Saghravani SF. 2018 Experimental study of the thermal conductivity features of the water based Fe_3O_4/CuO nanofluid. *Heat Mass Transfer.* **54**, 999–1008. (doi:10.1007/s00231-017-2188-z)

82. Syam Sundar L, Singh MK, Sousa ACM. 2013 Investigation of thermal conductivity and viscosity of Fe_3O_4 nanofluid for heat transfer applications. *Int. Commun. Heat Mass Transfer* **44**, 7–14. (doi:10.1016/j.icheatmasstransfer.2013.02.014)

83. Gao Y, Wang H, Sasmito AP, Mujumdar AS. 2018 Measurement and modeling of thermal conductivity of graphene nanoplatelet water and ethylene glycol base nanofluids. *Int. J. Heat Mass Transfer* **123**, 97–109. (doi:10.1016/j.ijheatmasstransfer.2018.02.089)

84. Akram N *et al.* 2019 An experimental investigation on the performance of a flat-plate solar collector using eco-friendly treated graphene nanoplatelets-water nanofluids. *J. Therm. Anal. Calorim.* **138**, 609–621. (doi:10.1007/s10973-019-08153-4)

85. Hajjar Z, Ghozatloo A. 2014 Enhanced thermal conductivities of graphene oxide nanofluids. *Int. Commun. Heat Mass Transfer* **57**, 128–131. (doi:10.1016/j.icheatmasstransfer.2014.07.018)

86. Sundar LS, Hortiguela MJ, Singh MK, Sousa ACM. 2016 Thermal conductivity and viscosity of water based nanodiamond (ND) nanofluids: an experimental study. *Int. Commun. Heat Mass Transfer* **76**, 245–255. (doi:10.1016/j.icheatmasstransfer.2016.05.025)

87. Yeganeh M, Shahtahmasebi N, Kompany A, Goharshadi EK, Youssefi A, Šiller L. 2010 Volume fraction and temperature variations of the effective thermal conductivity of nanodiamond fluids in deionized water. *Int. J. Heat Mass Transfer* **53**, 3186–3192. (doi:10.1016/j.ijheatmasstransfer.2010.03.008)

88. Pourhoseini SH, Naghizadeh N, Hoseinzadeh H. 2018 Effect of silver-water nanofluid on heat transfer performance of a plate heat exchanger: an experimental and theoretical study. *Powder Technol.* **332**, 279–286. (doi:10.1016/j.powtec.2018.03.058)

89. Bakhshan Y, Samari F, Ghaemi M, Ghafarigousheh S, Kakoee A. 2019 Experimental study on the thermal conductivity of silver nanoparticles synthesized using *Sargassum angostifolium*. *Iranian J. Sci. Technol. Trans. Mech. Eng.* **43**, 251–257. (doi:10.1007/s40997-018-0153-1)

90. Li Q, Xuan Y, Wang J. 2005 Experimental investigations on transport properties of magnetic fluids. *Exp. Therm Fluid Sci.* **30**, 109–116. (doi:10.1016/j.expthermflusci.2005.03.021)

91. Jin Kim H, Bang IC, Onoe J. 2009 Characteristic stability of bare Au-water nanofluids fabricated by pulsed laser ablation in liquids. *Opt. Lasers Eng.* **47**, 532–538. (doi:10.1016/j.optlaseng.2008.10.011)

92. Paul G, Pal T, Manna I. 2010 Thermo-physical property measurement of nano-gold dispersed water based nanofluids prepared by chemical precipitation technique. *J. Colloid Interface Sci.* **349**, 434–437. (doi:10.1016/j.jcis.2010.05.086)

93. Park J, Joo J, Kwon S, Jang Y, Hyeon T. 2007 Synthese monodisperser sphärischer Nanokristalle. *Angew. Chem.* **119**, 4714–4745. (doi:10.1002/ange.200603148)

94. Cushing BL, Kolesnichenko VL, O'Connor CJ. 2004 Recent advances in the liquid-phase syntheses of inorganic nanoparticles. *Chem. Rev.* **104**, 3893–3946. (doi:10.1021/cr030027b)

95. Chirico RD *et al.* 2013 Improvement of quality in publication of experimental thermophysical property data: challenges, assessment tools, global implementation, and online support. *J. Chem. Eng. Data* **58**, 2699–2716. (doi:10.1021/je400569s)

96. Nieto de Castro CA, Vieira SIC, Lourenço MJ, Murshed SMS. 2017 Understanding stability, measurements, and mechanisms of thermal conductivity of nanofluids. *J. Nanofluids* **6**, 804–811. (doi:10.1166/jon.2017.1388)

97. Nieto de Castro CA, Lourenço MJV. 2020 Towards the correct measurement of thermal conductivity of ionic melts and nanofluids. *Energies* **13**, 99. (doi:10.3390/en13010099)

98. Bobbo S, Buonomo B, Manca O, Vigna S, Fedele L. 2021 Analysis of the parameters required to properly define nanofluids for heat transfer applications. *Fluids* **6**, 65. (doi:10.3390/fluids6020065)

99. Brunelli A, Pojana G, Callegaro S, Marcomini A. 2013 Agglomeration and sedimentation of titanium dioxide nanoparticles (n-TiO$_2$) in synthetic and real waters. *J. Nanopart. Res.* **15**, 1684. (doi:10.1007/s11051-013-1684-4)

100. Singh BP, Jena J, Besra L, Bhattacharjee S. 2007 Dispersion of nano-silicon carbide (SiC) powder in aqueous suspensions. *J. Nanopart. Res.* **9**, 797–806. (doi:10.1007/s11051-006-9121-6)

101. Mingzheng Z, Guodong X, Jian L, Lei C, Lijun Z. 2012 Analysis of factors influencing thermal conductivity and viscosity in different kinds of surfactant solutions. *Exp. Therm Fluid Sci.* **36**, 22–29. (doi:10.1016/j.expthermflusci.2011.07.014)

102. Ali N, Teixeira JA, Addali A. 2018 A review on nanofluids: fabrication, stability, and thermophysical properties. *J. Nanomater.* **2018**, 6978130. (doi:10.1155/2018/6978130)

103. Sezer N, Atieh M, Koç M. 2018 A comprehensive review on synthesis, stability, thermophysical properties, and characterization of nanofluids. *Powder Technol.* **344**, 404–431. (doi:10.1016/j.powtec.2018.12.016)

104. Prasher R, Evans W, Meakin P, Fish J, Phelan P, Keblinski P. 2006 Effect of aggregation on thermal conduction in colloidal nanofluids. *Appl. Phys. Lett.* **89**, 143119. (doi:10.1063/1.2360229)

105. Jabbari F, Rajabpour A, Saedodin S. 2017 Thermal conductivity and viscosity of nanofluids: a review of recent molecular dynamics studies. *Chem. Eng. Sci.* **174**, 67–81. (doi:10.1016/j.ces.2017.08.034)

106. Tahmooressi H, Kasaeian A, Tarokh A, Rezaei R, Hoorfar M. 2020 Numerical simulation of aggregation effect on nanofluids thermal conductivity using the lattice Boltzmann method. *Int. Commun. Heat Mass Transfer* **110**, 104408. (doi:10.1016/j.icheatmasstransfer.2019.104408)

107. Gerardi C, Cory D, Buongiorno J, Hu LW, McKrell T. 2009 Nuclear magnetic resonance-based study of ordered layering on the surface of alumina nanoparticles in water. *Appl. Phys. Lett.* **95**, 253104. (doi:10.1063/1.3276551)

108. Thomä SLJ, Krauss SW, Eckardt M, Chater P, Zobel M. 2019 Atomic insight into hydration shells around facetted nanoparticles. *Nat. Commun.* **10**, 995. (doi:10.1038/s41467-019-09007-1)

109. Gawande MB, Goswami A, Felpin FX, Asefa T, Huang X, Silva R, Zou X, Zboril R, Varma RS. 2016 Cu and Cu-based nanoparticles: synthesis and applications in catalysis. *Chem. Rev.* **116**, 3722–3811. (doi:10.1021/acs.chemrev.5b00482)
110. Raudenbush SW. 2007 *HLM 6: hierarchical linear and nonlinear modeling*, 4th edn. Lincolnwood, IL: Scientific Software International.
111. Gelman A, Hill J. 2007 *Data analysis using regression and multilevel/hierarchical models*. Repr. with corr., 3. print. ed. Analytical methods for social research. Cambridge, UK: Cambridge University Press.